UCRL-20291
UC-48 Biology and Medicine
TID-4500 (57th Ed.)

TECHNIQUES FOR MAPPING THE SPATIAL DISTRIBUTION OF STOPPING π^- MESONS IN TISSUE

J. Sperinde, L. E. Temple, V. Perez-Mendez,
A. J. Miller and A. Rindi

March 3, 1971

AEC Contract No. W-7405-eng-48

LAWRENCE RADIATION LABORATORY
UNIVERSITY of CALIFORNIA BERKELEY

UCRL-20291

DISCLAIMER

Printed in the United States of America
Available from
Clearinghouse for Federal Scientific and Technical Information
National Bureau of Standards, U. S. Department of Commerce
Springfield, Virginia 22151
Price: Printed Copy $3.00; Microfiche $0.95

UCRL 20291

TECHNIQUES FOR MAPPING THE SPATIAL DISTRIBUTION OF STOPPING π^- MESONS IN TISSUE

J. Sperinde, L. E. Temple, V. Perez-Mendez, A. J. Miller and A. Rindi
Lawrence Radiation Laboratory
University of California
Berkeley, California

March 3, 1971

ABSTRACT

A number of processes leading to the emission of photons and neutrons in π^- capture reactions are discussed for potential use in radiation therapy to determine the stopping π^- region. It is concluded that the scheme of detecting collimated medium energy γ-rays is the most effective.

I. INTRODUCTION

Stopping π^- beams have been proposed [1] for radiotherapeutic applications since the "star" formation of the capture reaction produces a highly localized dense-ionization region, of high relative-biological-effectiveness. Highly ionizing radiation of this type is considered to be especially useful for the treatment of oxygen deficient tumors which are known to be less sensitive to radiation which has a low linear-energy-transfer. To insure that the pions come to rest in the tumor region an accurate monitor of the stopping pion distribution is desirable.

The lateral distribution and location of a stopping beam can be easily and reliably controlled with collimators and magnetic focusing and bending elements. A precise calculation of the stopping depth is

difficult because of the unknown density inhomogeneities in the patient. Hence the primary reason for a monitor is to determine the depth distribution.

Possible monitoring techniques reviewed in this paper include the use of:

1) Pi mesic x-rays; (2) Positron annihilation γ-rays; (3) Single γ-rays; (4) Neutrons; (5) γ-rays from neutral pion decay.

II. The Pion Capture Process

When a π^- comes to rest in matter, it is captured by the electric field of a nucleus. It then cascades through the atomic levels, emitting characteristic x-rays in the process, until it is absorbed by the nucleus. The capture process results in the emission of highly ionizing particles--star formation--as well as a number of neutrons and γ-rays. The neutron yield is approximately 3 per capture.[2] In approximately 2% of the events, radiative pion capture leads to the emission of γ-rays with an energy distribution which peaks around 100 MeV.[3] The residual nuclei following π^- capture are often left in excited states leading to the prompt emission of γ-rays in the energy range of a few MeV. The average excitation energy of the residual nuclei emitting γ-rays is calculated by Guthrie, et al.[4], to be about 5 MeV. A small percentage (approximately 1%) of the residual nuclei are positron unstable.[5] In water .2% of the pions are captured by hydrogen atoms.[6,7] Sixty percent of these pions charge exchange ($\pi^- + p \rightarrow \pi^o + n$) to form neutral pions with a momentum of 28.1 MeV/c. Since the π^o lifetime is 2×10^{-16} sec. the neutral pions decay in flight before interacting and in a distance

of less than 10^{-6} cm. Thus in contrast to positron annihilation, the relative angular distribution of the γ-rays from π^o decay has a spread of 20^o around 180^o.[6]

III. DISCUSSION OF MONITORING METHODS

1) Pi-mesic x-rays.

The 2p-1s pi-mesic transitions are potentially the most suitable of the pi-mesic x-rays for determining the pion stopping region.[8] Other transitions to the 1s level have much lower intensities. The x-rays from transitions between higher levels are attenuated more because they have less energy. Consider for instance pions captured by oxygen atoms - a very likely case in tissue. The 2p-1s transition has an energy of 159 KeV and occurs only 5% of the time[9] since nuclear absorption usually takes place before reaching the 1s level. This line is quite broad due to the short lifetime for nuclear capture. Pion beams always contain a small fraction of muons, typically from five to ten percent. The muons also produce x-rays in cascading through the atomic levels. The 3p-1s, 4p-1s, etc. muonic lines are superimposed on the broad pion 2p-1s line. Intensities of the muonic transitions are comparable to the pionic intensities, since the weakly interacting muons are all captured by the nucleus from the 1s level. There is also a large background of low energy photons, and higher energy photons Compton scattered in the detector. We show in fig. 1 the photon energy distribution in the pion stopping region for a 90 MeV π^- beam, and a water target. The beam consisted of 80% π^-, 10% μ^-, 10% e^-. The photons were detected with a 15 cc planar germanium detector[10], which was triggered on stopping pions and muons. As can be seen in the figure it is difficult to separate the pi-mesic

x-rays from the large background.

2) Positron annihilation γ-rays.

A possible system to detect the coincident γ-rays from positron annihilation which are emitted at 180° to each other is shown in fig. 2. It consists of multiwire proportional chambers on opposite sides of the stopping region. In front of each chamber is a thin lead converter. Assuming a conversion efficiency of 3%, a solid angle acceptance of 4.0 steradians, one positron per 100 stopping pions and a 50% probability that both of the annihilation γ-rays get out of the patient without interacting, we estimate a ratio of detected events to incident pions of 3×10^{-6}. This sensitivity can be increased tenfold by having three chambers with converters on each side of the stopping region, and should be sufficient to locate the stopping region with a minimal dose to the patient. Some work on the observation of the positron emitters following π^- absorption has been done by Taylor, et al.[5] They stopped a 100 MeV π^- beam in a stack of gelatin-filled plastic petri dishes. The positron activity of the individual petri dishes following irradiation was measured with a NaI detector. The results of their measurement are shown in fig. 3. As can be seen in the figure, the distribution of positron emitters gives a satisfactory representation of the π^- stopping distribution. There are, however, several disadvantages to using the positron emitters as a monitor of the stopping position. The lifetimes of the positron emitters [^{11}C(20.5 min), ^{13}N(9.96 min) and ^{15}O(2.07 min)] will introduce a time lag between the instantaneous change in the π^- stopping depth and its measurement by the detection of the positron annihilation γ-rays. The coincident detection of these γ-rays determines a point on each side of

the stopping region. The intersection of the line connecting these two points with the beam area is taken as the stopping π^- location. The position accuracy is limited by the size of the beam area, and the mean range of the positrons in tissue (about .25 cm for ^{11}C and ^{13}N and .5 cm for ^{15}O). Since the two γ-ray detectors will be unshielded there will be a background of charged particles. However the relatively long lifetimes of the positron emitters make it possible to avoid this background by gating-on the detector in the time interval between beam spills of the accelerator.

3) Single γ-rays.

(a) Method using a collimator. Gamma rays of energy greater than a few MeV travel through tissue with minimal scattering and attenuation. The pion stopping distribution can be determined by collimating and converting the gamma rays to electrons and detecting the electrons with a position sensitive detector.

This technique was employed by Sperinde, et al.[11] The experimental set-up is shown in fig. 4a. The π^- beam was stopped in an absorber of lucite. The collimator consisted of 1.5 mm. sheets of lead separated by 1.5 mm. air gaps, with a 3 mm. thick lead converter. An aluminum absorber was used to put a low energy cutoff on the detected electrons. The coincidence signal from a pair of scintillators, one between the converter and the spark chamber, the other behind the aluminum absorber triggered the spark chamber. The spark locations were read out electronically and stored in a pulse-height analyzer. We show the results in fig. 5, curve A, for a beam stopping in lucite and a 2.5 cm thick Al absorber. The solid line is a least-squares fit to the data assuming

a gaussian peak. The dashed line is a depth-dose curve measured with an ionization chamber, normalized to the same peak height. As can be seen from the figure, the background is low and the agreement between the ionization chamber results and the γ-ray measurement is quite good. The ratio of detected γ-rays to incident pions is 5×10^{-6}. This sensitivity is sufficient to locate the stopping region with a small dose to the patient. The sensitivity can be increased if needed by increasing the size of the system and improving the design of the collimator.

We measured the resolution of the system by observing the γ-rays produced in a .6 cm thick sheet of lucite. The results can be seen in fig. 6. The solid line is a least squares fit to the data. The full width at half-maximum of the peak is 1 cm. Correcting for the thickness of the lucite, the measurement gives a spatial resolution of .75 cm full width at half maximum.

The electrons produced in the lead converter scatter in passing through the lead. This gives an angular spread to the converted electrons and limits the spatial resolution of the system. The spatial resolution can be improved by collimating the converted electrons as shown in fig. 4b.

One can vary the cutoff energy of the electrons, and thus the cutoff energy of the γ-rays by changing the thickness of the aluminum absorber. An aluminum absorber thickness of 2.5 cm corresponds to the range of a 15 MeV electron. In fig. 5, curve B, we show the results for a .6 cm (approximately 4 MeV electron) aluminum absorber. As can be seen from the figure, the low energy electrons merely increase the background.

The location of the electrons in the system described above was determined with a magnetostrictive readout wire spark chamber.(12) However

this is not essential to the system and in the future we would propose to use a multiwire proportional chamber[13] with delay line readout.[14] This would give an increased data acquisition rate, and simplify the electronics by making the high-voltage pulsing apparatus and one of the triggering scintillators unnecessary. Such a system could also be used to determine the stopping location in tissue of alphas and protons since nuclear interactions in the tissue will leave some of the residual nuclei in excited states, which decay by prompt γ-ray emissions. The threshold for nuclear excitation via proton or alpha bombardment is approximately 10 MeV. The residual range of these particles is less than 1 mm. Work to determine the spatial distribution of prompt γ-rays from stopping alphas is now in progress.

(b) Method using a pair of chambers without collimator. The π^- stopping position might also be located by determining the γ-ray position and direction. The intersection of the extrapolated γ-ray direction with the beam area indicates the π^- stopping location with a spatial resolution limited by the size of the beam area and the precision with which the γ-ray direction is determined. The γ-ray is converted in a thin foil and the direction of the electron can be determined with two wire chambers spaced a few centimeters apart. This method has the advantage of not needing a collimator and thus it is possible to obtain a large increase in solid angle acceptance. However the conversion efficiency is low since the converter must be very thin to minimize scattering so that the converted electrons accurately preserve the direction of the incident γ-rays. Assuming an average γ-ray energy of 100 MeV, there is a .5 probability[15] that both secondary electrons have energies greater than 25 MeV. The rms angular spread for 25 MeV secondary electrons following pair

production is .05 radians. A lead converter of approximately .045 gm/cm^2 gives rms angular spread due to multiple scattering of approximately .05 radians and has a conversion efficiency of approximately 4×10^{-3}. For a detector 25 cm from the stopping pion region subtending a solid angle of approximately 2.1 steradians the spatial resolution neglecting uncertainties due to the size of the beam area is approximately 1.7 cm and the sensitivity is approximately 1.3×10^{-5} detected γ-rays per incident pion.

The sensitivity for such a system is more than sufficient to map the stopping pion distribution, but the spatial resolution is marginal. Also, since the system is not shielded there will be a charged particle background.

4) Neutrons.

The neutron yield following π^- capture is approximately 100 times greater than the high energy γ-ray yield. A determination of the direction of these neutrons could be used to find the π^- stopping region using a system similar to that used to detect collimated γ-rays. In this case the collimator and the converter would probably be made of polyethelyne and the recoil protons produced as a result of neutron-proton collisions would be detected. However the collimation of neutrons is appreciably more difficult than the collimation of γ-rays due to the longer mean free path of neutrons in matter. In our opinion this collimation problem makes the method impractical.

5) γ-rays from neutral pion decay.

The coincident detection of both of the γ-rays from the decay of neutral pions can potentially give a three dimensional representation of the stopping distribution.(16) The direction of both γ-rays must be

determined, and their intersection point found. The direction of the individual γ-rays can be determined with the same system discussed earlier for detection of single γ-rays, with one detector on each side of the stopping region. The coincident detection of both γ-rays allows one to discriminate electronically against charged particle background. In addition to the limitations discussed in Section 3(b) there is a decrease in sensitivity of 4×10^{-3} due to the need for an additional converter. Increasing the sensitivity by making the converter thicker would result in a degraded spatial resolution due to increased multiple scattering of the secondary electrons.

CONCLUSION

From the discussion above, it can be seen that any one of the various methods could be used to provide some information on the stopping π^- distribution in vivo. Our own experience in some of these, coupled with numerical estimates on all of them, leads us to the conclusion that the detection of moderately high energy γ-rays, defined through a multi-slot collimator offers the maximum reliability as well as being potentially the most accurate method.

If necessary, this method could be supplemented by measuring the distribution of annihilation γ-rays from the induced positron activity after the termination of the bombardment period.

As far as the detection of the converted electrons is concerned, a spark chamber, wire proportional chamber or any other device capable of identifying the particular slot through which a γ-ray passes would be satisfactory. In the present stage of technological development, we favor the use of multi-wire proportional chambers with a digitized electronic read-out.

FOOTNOTE AND REFERENCES

* This work was done under the auspices of the U. S. Atomic Energy Commission.

1) P. H. Fowler and D. H. Perkins, Nature, 189 (1961) 524; C. Richman, H. Aceto Jr., M. R. Raju, and B. Schwartz, Am. J. Roentgenol, 96 (1966) 777.

2) P. H. Fowler and V. M. Mayes, Proc. Phys. Soc. 92 (1961) 377.

3) H. Davies, H. Muirhead and J. N. Woulds, Nucl. Phys., 78 (1966) 673.

4) M. P. Guthrie, R. G. Alsmiller, Jr. and H. W. Bertini, Nucl. Inst. and Methods, 66 (1968) 29.

5) M. C. Taylor, G. C. Phillips, R. C. Young, Science, 169 (1970) 377.

6) V. I. Petrukhin and Yu D. Prokoshkin, Nuovo Cimento, 28 (1963) 99.

7) M. Chabre, P. Depommier, J. Heintze and V. Soergel, Phys. Lett., 5 (1963) 67.

8) Louis Rosen, Nuclear Applications, 5 (1968) 379.

9) H. Koch, G. Poelz, H. Schmitt, L. Tauscher, G. Backenstoss, S. Charalambus, and H. Daniel, Phys. Lett., 28B (1968) 278.

10) Fred S. Goulding, Nucl. Inst. and Methods, 43 (1966) 1.

11) J. Sperinde, V. Perez-Mendez, A. J. Miller, A. Rindi, and M. R. Raju, Phys. Med. Biol., 15 (1970) 643.

12) V. Perez-Mendez and J. M. Pfab, Nucl. Inst. and Methods, 33 (1965) 141.

13) G. Charpak, R. Bouclier, T. Bressani, J. Favier and C. Zupancic, Nucl. Inst. and Methods, 62 (1968) 262; 65 (1968) 217.

14) A. Rindi, V. Perez-Mendez and R. I. Wallace, Nucl. Inst. and Methods, 77 (1970) 325; R. Grove, K. Lee, V. Perez-Mendez and J. Sperinde, Nucl. Inst. and Methods, 89 (1970) 257.

15) Bruno Rossi, High Energy Particles, Prentice-Hall, New York, 1952.

16) A. Schwettman and D. Body, private communication.

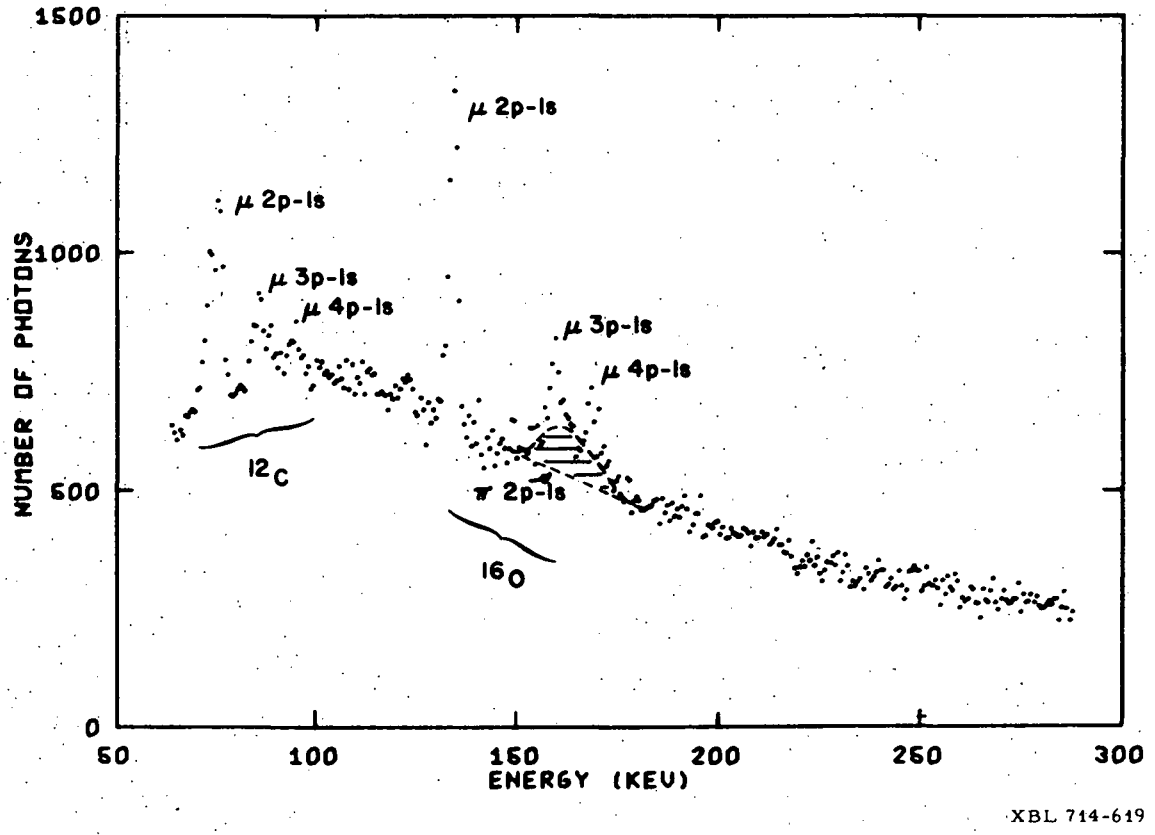

Fig. 1. The number of low energy photons detected plotted as a function of photon energy for a 90 MeV π^- beam stopping in a water target. The carbon lines are due to the lucite container which holds the water.

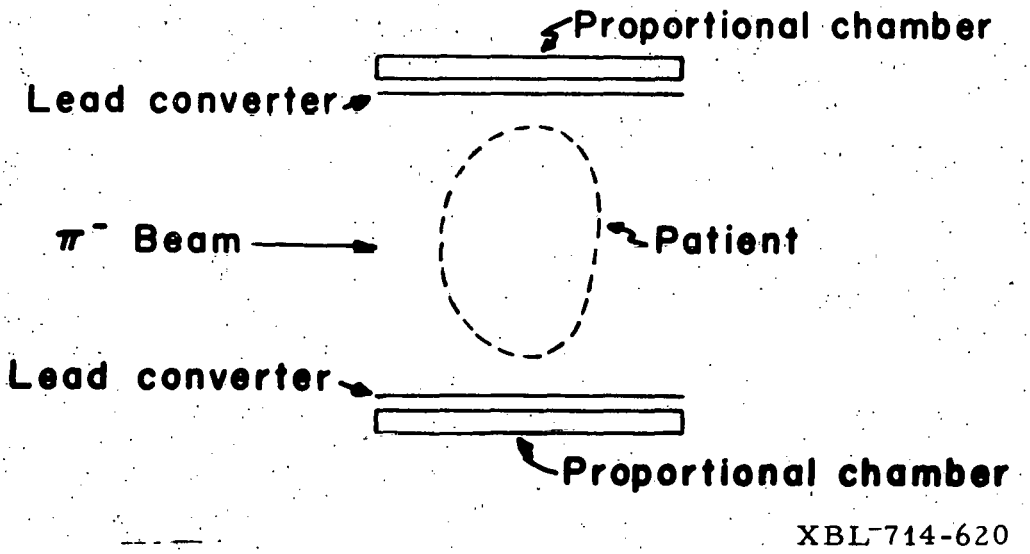

Fig. 2. Setup for detecting coincident back-to-back γ-rays from positron annihilation.

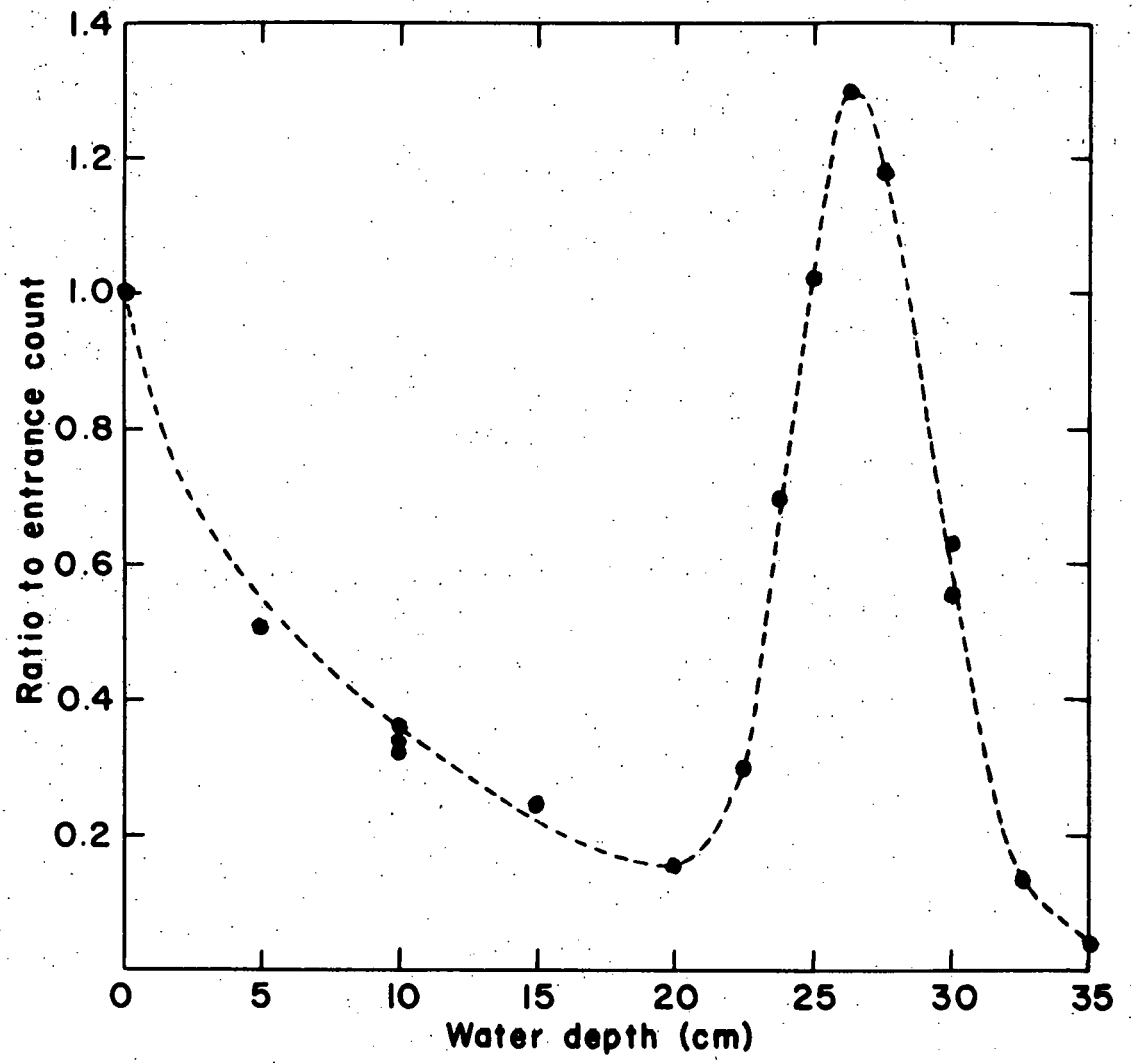

XBL 714-618

Fig. 3. The relative yield of positron emitters as a function of depth for 100 MeV negative pions in water.

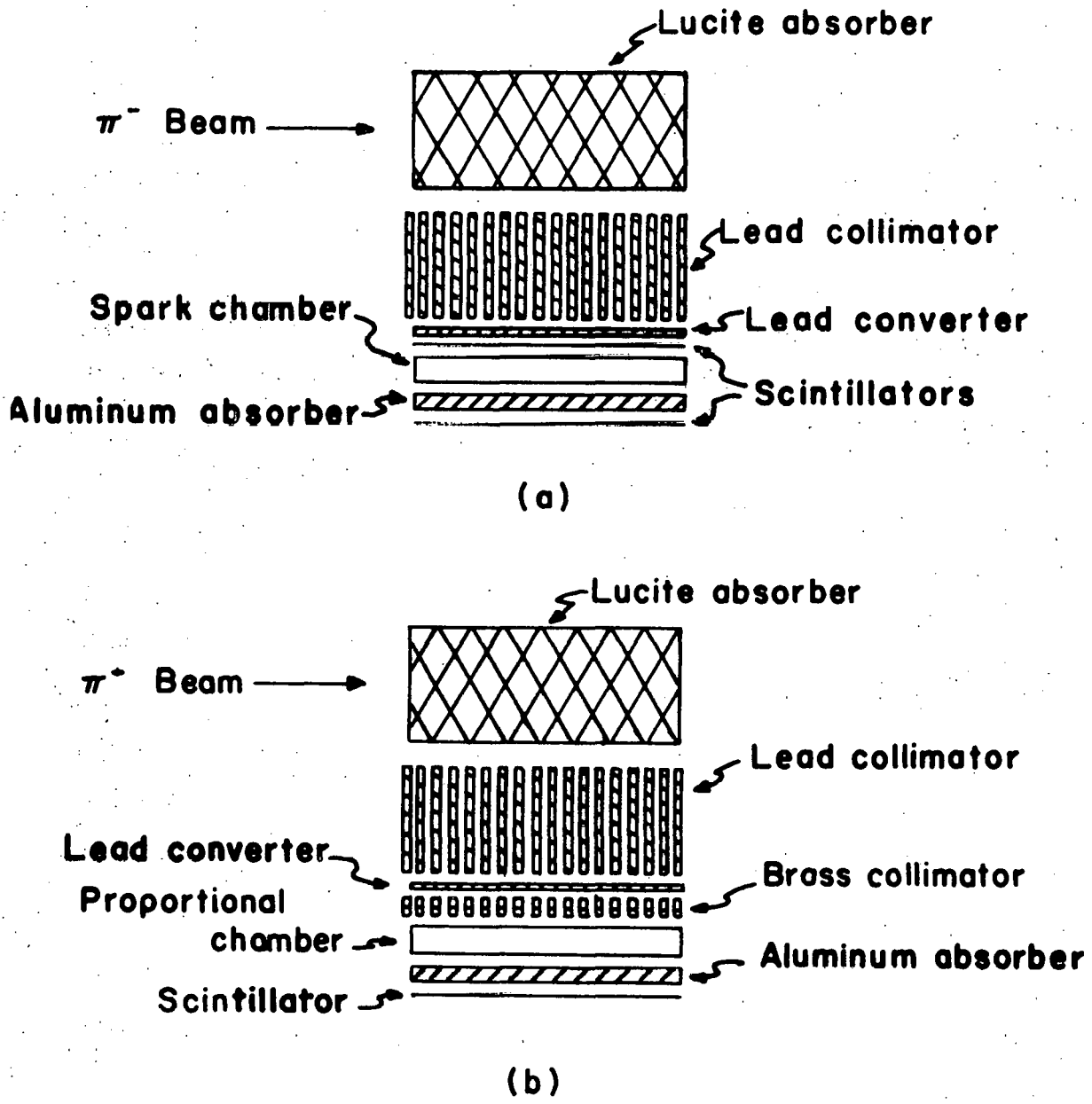

XBL 714-616

Fig. 4. Set-up for detecting single collimated γ-rays: (a) apparatus used in reported measurements (b) apparatus proposed for future work.

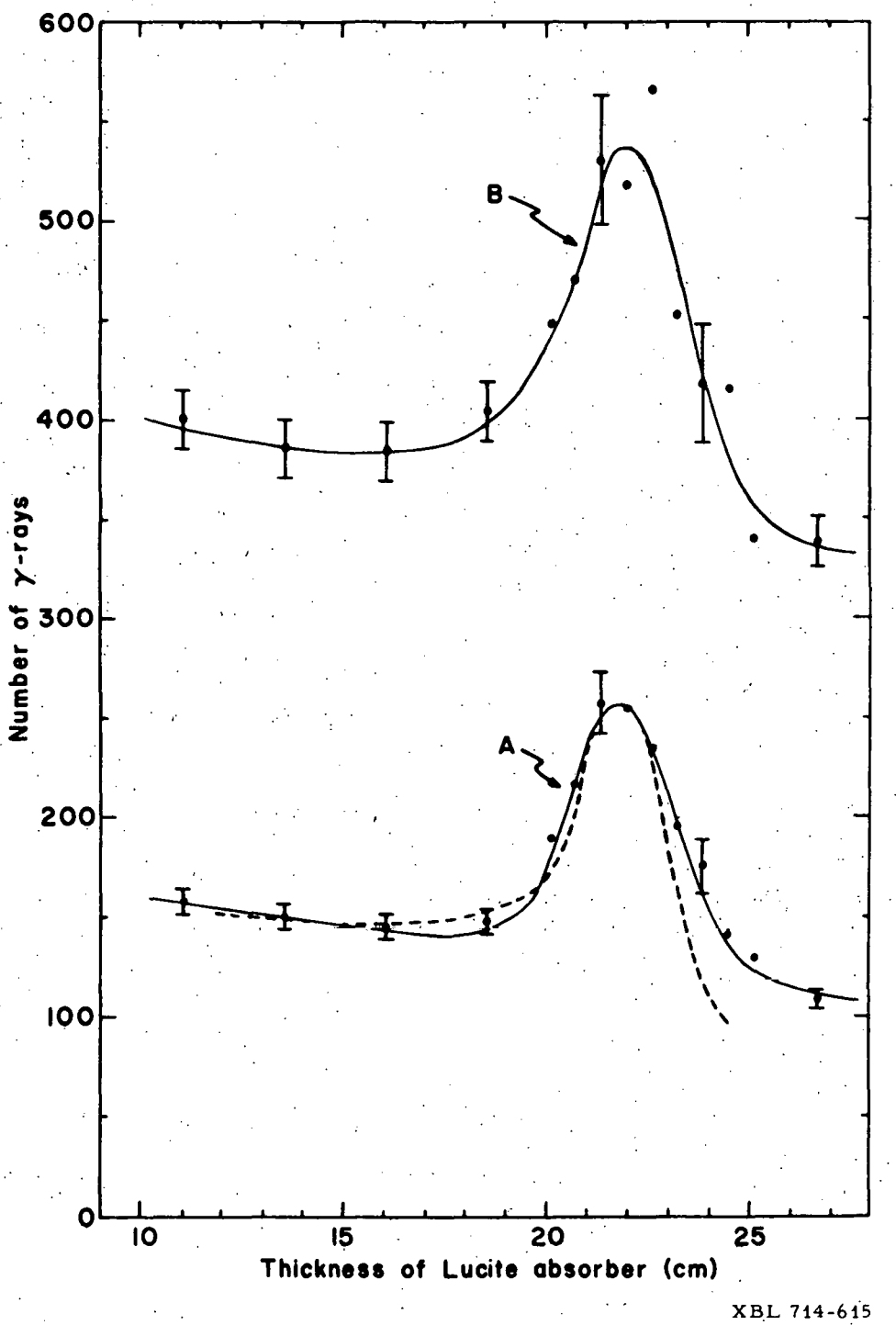

Fig. 5. The number of γ-rays detected as a function of depth in lucite with A: 2.5 cm of aluminum absorber and B: .6 cm of aluminum absorber. The dashed line is a depth-dose curve measured with an ionization chamber normalized to the same peak height as curve A.

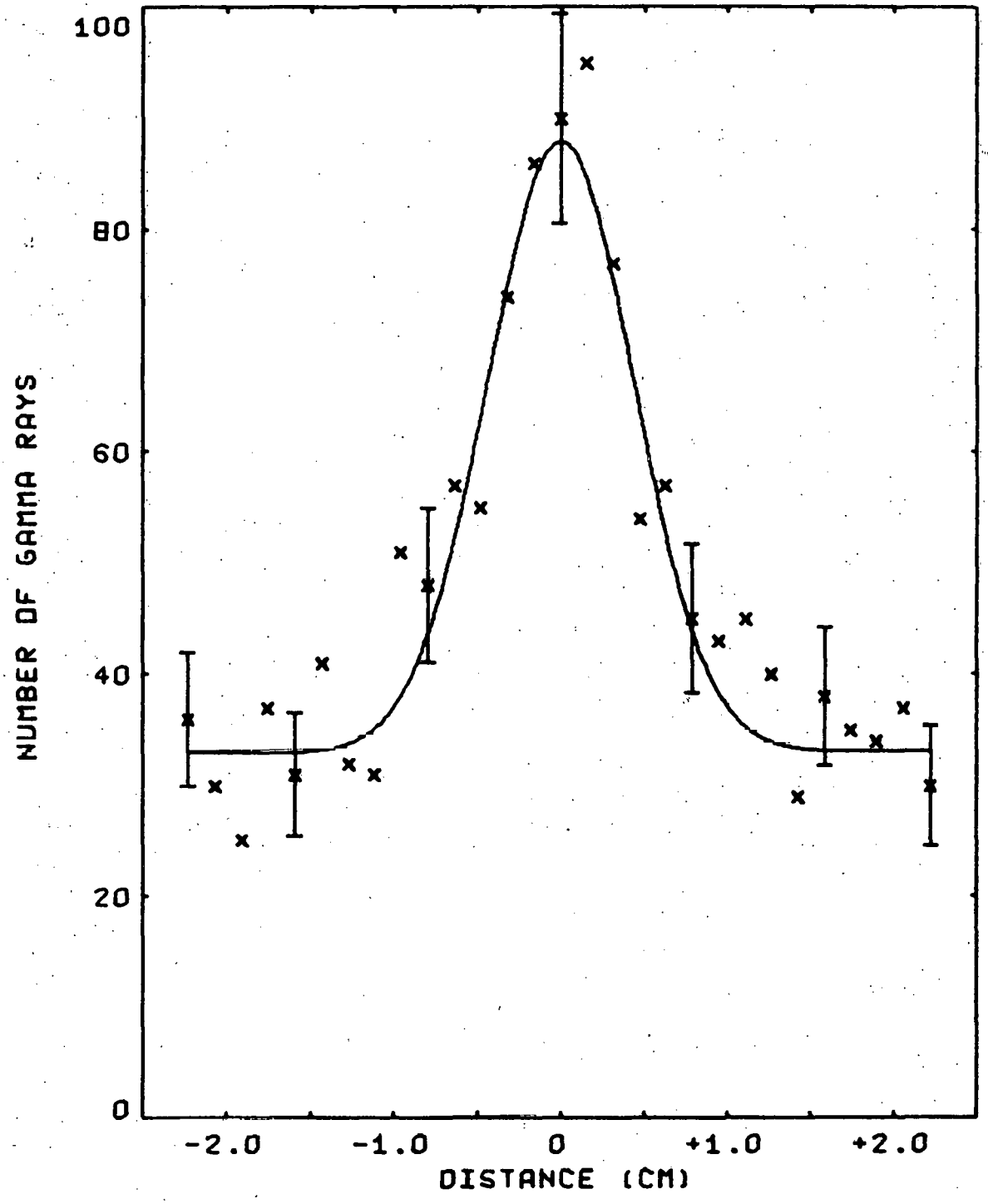

XBL 714-617

Fig. 6. Number of γ-rays detected as a function of position with the pion beam incident on a .6 cm thick sheet of lucite. The solid curve is a least-squares fit to the data assuming a gaussian peak superimposed on a uniform background.

TECHNICAL INFORMATION DIVISION
LAWRENCE RADIATION LABORATORY
UNIVERSITY OF CALIFORNIA
BERKELEY, CALIFORNIA 94720